

# Dalton Transactions

Accepted Manuscript



This is an *Accepted Manuscript*, which has been through the Royal Society of Chemistry peer review process and has been accepted for publication.

*Accepted Manuscripts* are published online shortly after acceptance, before technical editing, formatting and proof reading. Using this free service, authors can make their results available to the community, in citable form, before we publish the edited article. We will replace this *Accepted Manuscript* with the edited and formatted *Advance Article* as soon as it is available.

You can find more information about *Accepted Manuscripts* in the [Information for Authors](#).

Please note that technical editing may introduce minor changes to the text and/or graphics, which may alter content. The journal's standard [Terms & Conditions](#) and the [Ethical guidelines](#) still apply. In no event shall the Royal Society of Chemistry be held responsible for any errors or omissions in this *Accepted Manuscript* or any consequences arising from the use of any information it contains.



Journal Name

ARTICLE

## Interactions Between the Trianionic Ligand-centred Redox-active Metalloligand $[\text{Cr}^{\text{III}}(\text{perfluorocatecholato})_3]^{3-}$ and Guest Metal Ions

Received 00th January 20xx,  
Accepted 00th January 20xx

DOI: 10.1039/x0xx00000x

www.rsc.org/

Masanori Wakizaka,<sup>a, b</sup> Takeshi Matsumoto,<sup>b</sup> Atsushi Kobayashi,<sup>a</sup> Masako Kato,<sup>\*, a</sup> and Ho-Chol Chang<sup>\*, b</sup>

The redox-active metalloligand (RML)  $(\text{Et}_3\text{NH})_3[\text{Cr}^{\text{III}}(\text{F}_4\text{Cat})_3]$  ( $\text{F}_4\text{Cat}$  = perfluorocatecholato) (**1**) was synthesized and its interactions with the guest metal ions  $\text{Li}^+$ ,  $\text{Mn}^{2+}$ ,  $\text{Fe}^{2+}$ ,  $\text{Co}^{2+}$ ,  $\text{Cu}^{2+}$ , and  $\text{Zn}^{2+}$  were examined. Cyclic voltammetry measurements and spectroelectrochemical studies revealed that complex **1** shows three-step ligand-centred one-electron oxidations to consecutively generate  $[\text{Cr}^{\text{III}}(\text{F}_4\text{Cat})_2(\text{F}_4\text{SQ})]^{2-}$  ( $\text{F}_4\text{SQ}$  = perfluorosemiquinonato),  $[\text{Cr}^{\text{III}}(\text{F}_4\text{Cat})(\text{F}_4\text{SQ})]^-$ , and  $[\text{Cr}^{\text{III}}(\text{F}_4\text{SQ})_3]$  at  $-0.12$ ,  $0.23$ , and  $0.53$  V vs.  $\text{Ag}/\text{Ag}^+$  in dichloromethane, or at  $-0.21$ ,  $0.08$ , and  $0.50$  V in acetonitrile (MeCN), respectively. Titration experiments in MeCN revealed that treatment of **1** with  $\text{Cu}^{2+}$  leads to the formation of  $[\text{Cr}^{\text{III}}(\text{F}_4\text{Cat})_2(\text{F}_4\text{SQ})]^{2-}$  and  $\text{Cu}^+$  *via* a redox reaction. However, when **1** was treated with  $\text{Li}^+$ ,  $\text{Mn}^{2+}$ ,  $\text{Fe}^{2+}$ ,  $\text{Co}^{2+}$ , and  $\text{Zn}^{2+}$ , further titration experiments revealed that these metal ions coordinated *via* the lone pairs on the coordinating oxygen atoms of the  $\text{F}_4\text{Cat}^{2-}$  moieties in a one-to-one ratio, and the binding constants of  $3.7 (\pm 0.3) \times 10^4$  ( $\text{Li}^+$ ),  $1.5 (\pm 0.2) \times 10^5$  ( $\text{Mn}^{2+}$ ),  $2.2 (\pm 0.4) \times 10^5$  ( $\text{Fe}^{2+}$ ),  $1.9 (\pm 0.2) \times 10^5$  ( $\text{Co}^{2+}$ ), and  $3.8 (\pm 0.4) \times 10^5 \text{ M}^{-1}$  ( $\text{Zn}^{2+}$ ) were established. Moreover, the oxidation potentials of **1** were positively shifted by  $0.08$ – $0.33$  V upon addition of guest metal ions. Spectroelectrochemical studies of **1** in the presence of guest metal ions suggested that ligand-centred one- and two-electron oxidation of the RML occurred for  $\text{Li}^+$ ,  $\text{Mn}^{2+}$ ,  $\text{Co}^{2+}$ , and  $\text{Zn}^{2+}$ , respectively, while guest metal-centred one-electron oxidation was observed for  $\text{Fe}^{2+}$ . Considering all the aforementioned results, this study demonstrated for the first time the ability of  $[\text{Cr}^{\text{III}}(\text{F}_4\text{Cat})_3]^{3-}$  to act as a RML in solution.

### Introduction

The development of molecules and/or supramolecular assemblies that exhibit multi-electron transfer is an attractive research target not only in basic chemistry but also in advanced chemistry, including catalytic substrate conversions *via* redox reactions.<sup>1</sup> So far, several types of multi-electron transfer molecules have been reported, *e.g.*,  $\pi$ -conjugated organic compounds,<sup>2</sup> polyoxometalates,<sup>3</sup> and metal complexes<sup>4</sup> containing redox-active metals. For example, ferrocene is one of the most useful transition metal complexes, demonstrating “metal-centred” one-electron transfer reactions.<sup>5</sup> Supramolecular assemblies such as hexaferrocenylbenzene or ferrocenyl dendrimers have also been reported to show multi-electron transfer reactions on

the Fe(II) centres of each ferrocenyl moiety.<sup>5</sup> Ito and Yamaguchi *et al.* reported a dodeca-nuclear Ru complex consisting of four  $[\text{Ru}_3\text{O}(\text{CH}_3\text{CO}_2)_6]$  units linked *via* bridging pyrazine ligands, which exhibits a 14-step-15-electron transfer reaction on the Ru centres.<sup>6</sup> These examples have demonstrated that the aggregation of multiple redox-active metal centres can be regarded as a powerful method for the creation of multi-electron transfer systems.

In addition to the aforementioned metal-centred electron transfer processes, the corresponding ligand-centred processes have also been studied, so far.<sup>7</sup> For instance, catechol ( $\text{CatH}_2$ ),<sup>8</sup> 2-benzenedithiol ( $\text{BdtH}_2$ ),<sup>9</sup> and 2-mercaptophenol ( $\text{MpH}_2$ )<sup>10</sup> have been reported to coordinate to transition metal ions, and to exhibit both metal- and ligand-centred redox reactions. Especially, the redox properties of tris-  $\text{Cat}/\text{SQ}$  ( $\text{SQ}$  = semiquinonato) complexes, have been well established.<sup>11</sup> For example,  $[\text{Re}^{\text{VI}}(\text{Cl}_4\text{Cat})_3]$  shows two-step metal-centred  $\text{Re}^{\text{VI}}/\text{Re}^{\text{V}}/\text{Re}^{\text{IV}}$  redox couples,<sup>12</sup> while  $[\text{Cr}^{\text{III}}(\text{X}_4\text{SQ})_3]$  ( $\text{X} = \text{Cl}$  and  $\text{Br}$ ) exhibits three-step ligand-centred  $\text{Cat}/\text{SQ}$  redox couples as shown in Scheme 1.<sup>13</sup>

Here we noted that  $\text{Cat}$  complexes may be used as metalloligands (MLs)<sup>14</sup> that bind to guest metal ions *via* the lone pairs on the coordinating oxygen atoms of the ligands as shown in Chart 1. Previously reported  $[\text{K}_3(\text{H}_2\text{O})_{1.5}\{\text{M}^{\text{III}}(\text{Cat})_3\}]_n$

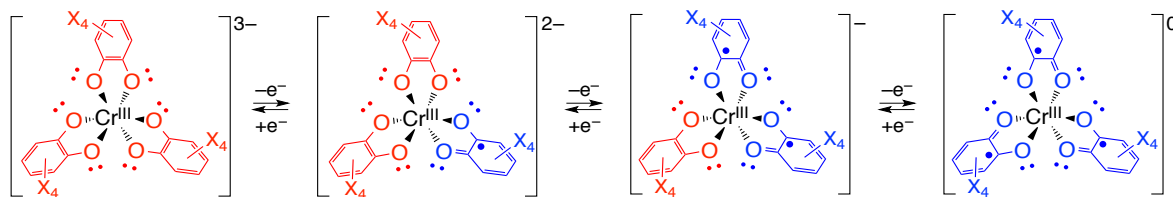
<sup>a</sup> Division of Chemistry, Faculty of Science, Hokkaido University, North-10, West-8, Kita-ku, Sapporo 060-0810, Japan.

<sup>b</sup> Department of Applied Chemistry, Faculty of Science and Engineering, Chuo University, 1-13-27 Kasuga, Bunkyo-ku, Tokyo 112-8551, Japan.

\* To whom correspondence should be addressed. E-mail: chang@kc.chuo-u.ac.jp. Phone: +81-3-3817-1897. Fax: +81-3-3817-1895.

Electronic Supplementary Information (ESI) available: The ESI contains the ESI-MS spectra, CVs, electrochemical data,  $v^{1/2}$  versus  $\Delta E$  plots, UV-vis-NIR spectra, and the spectroelectrochemical data. See DOI: 10.1039/x0xx00000x

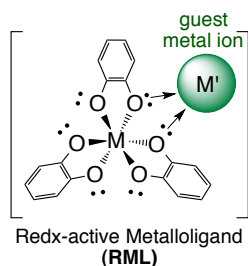
Dalton Transactions Accepted Manuscript

**Scheme 1.** Scheme for the redox processes in  $[\text{Cr}^{\text{III}}(\text{X}_4\text{SQ})_3]$  ( $\text{X} = \text{Cl}$  and  $\text{Br}$ )<sup>9b, 9c</sup>

( $\text{M} = \text{Cr}$  and  $\text{Fe}$ ),<sup>15a</sup>  $[\text{K}_3\{\text{V}^{\text{III}}(\text{Cat})_3\}]_n$ ,<sup>15b</sup>  $[\text{Li}_2(\text{C}_4\text{H}_8\text{O})_4\{\text{Mn}^{\text{III}}(\text{Br}_4\text{Cat})_3\}]^-$ ,<sup>15c</sup> and  $[\text{K}_2(\text{MeCN})_6\{\text{Mn}^{\text{IV}}(3,5\text{-DTBCat})_3\}]$  (3,5-DTBCat = 3,5-di-*tert*-butylcatecholato)<sup>15d</sup> exhibited binding interactions between the oxygen atoms of the Cat<sup>2-</sup> moieties and alkaline metal ions. Although the molecular structures of these complexes in the crystalline state have been published, details on their physicochemical properties in solution remain to be reported. One of our previous studies demonstrated that  $[\text{Mo}^{\text{V}}(\text{Bdt})_3]^-$ , with metal-centred redox properties, is able to capture soft  $\text{Cu}^+$  and  $\text{Ag}^+$  ions by interaction with the lone pairs on the sulphur atoms, resulting in the formation of 1-D chains and 3-D network structures in the solid state.<sup>16</sup> Moreover, we reported that *fac*- $[\text{Mo}^{\text{V}}(\text{Mp})_3]^-$ , a redox-active metalloligand (RML) with possible coordination sites at the oxygen and sulphur atoms, exhibits a site-dependent binding of guest metal ions such as  $\text{Na}^+$ ,  $\text{Mn}^{2+}$ ,  $\text{Fe}^{2+}$ ,  $\text{Co}^{2+}$ , and  $\text{Ni}^{2+}$  on the oxygen sites, while  $\text{Cu}^+$  is coordinated at the sulphur sites.<sup>17</sup> It is noteworthy that the binding of the metal ions at the oxygen sites of the RML, leads to an enhancement of the electron-accepting properties of the RML, *i.e.* the reduction potential of the thus obtained complex is positively shifted by approximately 0.6 V relative to that of the guest metal-free RML in solution. These studies thus indicate that the redox properties of RML(s) may be modulated in solution by interactions with guest metal ions even in solution.

Even though binding properties of metal-centred RMLs with guest metal ions have been reported,<sup>16, 17</sup> those of ligand-centred RMLs have not been reported so far; neither in solution, nor in the solid state. The combination of the ligand-centred redox function of the RML and the chemical properties of guest metal ions may allow the design of novel functional assemblies, in which ligands act as electron/hole reservoirs.

In this study, we aimed to unveil the interactions between ligand-centred RMLs and guest metal ions. For that purpose, we designed the RML  $(\text{Et}_3\text{NH})_3[\text{Cr}^{\text{III}}(\text{F}_4\text{Cat})_3]$  ( $\text{F}_4\text{Cat} =$  perfluorocatecholato) (**1**) as an alternative multi-electron transfer system. In order to increase its electron-accepting

**Chart 1.** Representative structure for an assembly consisting of an RML and a guest metal ion.

properties, perfluoro-groups were introduced in the Cat ligands, as they combine stronger electron-withdrawing properties with smaller atom size relative to perchloro and perbromo groups.<sup>18</sup> Herein, we discuss the synthesis and redox properties of **1** as well as its interactions with the guest metal ions  $\text{Li}^+$ ,  $\text{Mn}^{2+}$ ,  $\text{Fe}^{2+}$ ,  $\text{Co}^{2+}$ ,  $\text{Cu}^{2+}$ , and  $\text{Zn}^{2+}$ , that differ in charge and redox properties.

## Experimental Section

**General Procedures.** All synthetic operations were performed under an atmosphere of  $\text{N}_2$  using Schlenk-line techniques. The compounds  $\text{CrCl}_3 \cdot 6\text{H}_2\text{O}$ ,  $\text{LiClO}_4$ ,  $\text{M}(\text{ClO}_4)_2 \cdot 6\text{H}_2\text{O}$  ( $\text{M} = \text{Mn}, \text{Fe}, \text{Co}, \text{Cu},$  and  $\text{Zn}$ ), and benzene were purchased from Wako Pure Chemical Industries. Anhydrous solvents, methanol ( $\text{MeOH}$ ), acetonitrile ( $\text{MeCN}$ ), dichloromethane ( $\text{CH}_2\text{Cl}_2$ ), and *n*-hexane, were purchased from Kanto Chemical Co. Inc.. Triethylamine ( $\text{Et}_3\text{N}$ ) was purchased from Tokyo Kasei Kogyo Co. Ltd. Perfluorocatechol ( $\text{F}_4\text{CatH}_2$ ),<sup>19</sup>  $[\text{Cr}^{\text{III}}(\text{X}_4\text{SQ})_3]$  ( $\text{X} = \text{Cl}$  and  $\text{Br}$ ),<sup>13b</sup> and  $[\text{Cu}(\text{MeCN})_4]\text{PF}_6$ <sup>20</sup> were synthesized according to literature procedures. All solvents were degassed by at least five freeze-pump-thaw cycles immediately prior to use. **Caution!** Although we did not experience any difficulties with the perchlorate salts, these should be regarded as potentially explosive, and therefore be handled with the utmost care.

**Synthesis of  $(\text{Et}_3\text{NH})_3[\text{Cr}^{\text{III}}(\text{F}_4\text{Cat})_3]$  (**1**).** A colourless 5 mL  $\text{MeOH}$  solution of  $\text{Et}_3\text{N}$  (333 mg, 3.30 mmol) was added to a green 15 mL  $\text{MeOH}$  solution of  $\text{CrCl}_3 \cdot 6\text{H}_2\text{O}$  (147 mg, 0.55 mmol) and  $\text{F}_4\text{CatH}_2$  (300 mg, 1.65 mmol). Upon mixing the two solutions, a green suspension was formed immediately. After continuous stirring for 12 h, the green precipitate dissolved to afford a green solution. After removing  $\text{MeOH}$  under reduced pressure, the product was extracted with 8 mL benzene, and a white by-product was filtered off, affording a green benzene solution. Addition of 16 mL *n*-hexane to this solution afforded a green powder. After filtration, the powder was washed three times with each 3 mL *n*-hexane and dried *in vacuo*; complex **1** was isolated as green powder in 60% yield. Anal. Found: C, 48.14; H, 5.59; N, 4.56. Calcd. for  $\text{C}_{36}\text{H}_{48}\text{CrF}_{12}\text{N}_3\text{O}_6$  (**1**): C, 48.11; H, 5.38; N, 4.68. ESI-MS ( $m/z$ ): Calcd for  $[\mathbf{1}+\text{H}]^+$ : 899.28; found: 899.31.

**Physical Measurements.** Elemental analyses were carried out at the analysis centre of Hokkaido University. Cyclic voltammetry measurements were recorded with a BAS model 650A electrochemical analyser, using a glassy carbon (GC) working electrode and a platinum (Pt) auxiliary electrode under an atmosphere of argon (Ar). The reference electrode consisted of a silver wire, inserted into a small glass tube fitted with a porous Vycor frit at the tip, filled with a  $\text{MeCN}$  solution containing 0.1 M *n*- $\text{Bu}_4\text{NClO}_4$  and 0.01 M  $\text{AgNO}_3$ . All three

electrodes were immersed in 2 mL of a  $\text{CH}_2\text{Cl}_2$  or MeCN solution containing 0.1 M  $n\text{-Bu}_4\text{NPF}_6$  as the supporting electrolyte and the analytes. In all cases, redox potentials were measured relative to the  $\text{Ag}/\text{Ag}^+$  redox couple. UV-Vis-NIR spectra were recorded on a Hitachi U-4100 spectrophotometer over the range 200–3300 nm at 296 K under an atmosphere of  $\text{N}_2$ . Spectroelectrochemical measurements were carried out in 0.1 M  $n\text{-Bu}_4\text{NPF}_6$  solution using Pt, Pt mesh, and the reference electrodes under an atmosphere of  $\text{N}_2$ . Electrospray ionization mass (ESI-MS) spectra were recorded on a JEOL JMS-T100LC AccuTOF spectrometer under an atmosphere of  $\text{N}_2$ .

## Results and Discussion

### Synthesis and Characterisation of **1**.

Two tris-Cat Cr(III) complexes,  $\text{K}_3[\text{Cr}^{\text{III}}(\text{Cat})_3]^{15\text{a}, 21\text{a}}$  and  $\text{K}_3[\text{Cr}^{\text{III}}(3,5\text{-DTBCat})_3]^{21\text{b}}$  have previously been reported by Raymond *et al.* These complexes were synthesized in aqueous solution by the treatment of Cr(III) chloride or acetate with three equivalents of  $\text{CatH}_2$  or 3,5-DTBCat $\text{H}_2$  in the presence of an excess of KOH under an inert atmosphere, and the products were isolated as green solids. Complex **1** was obtained in a similar fashion from the treatment of  $\text{CrCl}_3 \cdot 6\text{H}_2\text{O}$  with three equivalents of  $\text{F}_4\text{CatH}_2$  in MeOH in the presence of six equivalents of  $\text{Et}_3\text{N}$  under an atmosphere of  $\text{N}_2$ . Similarly to the previously reported tris-Cat Cr(III) complexes,<sup>15a, 21</sup> complex **1** was isolated as a green solid. A positive-mode ESI-MS spectrum of the product showed the main peak at  $m/z = 899.31$  (Figures 1a and S1a), which is consistent with the exact mass of  $\{(\text{Et}_3\text{NH})_3[\text{Cr}(\text{C}_6\text{F}_4\text{O}_2)_3] + \text{H}^+\}^+$  (899.28). Moreover, the analysis of the elemental composition for **1** supports the assigned formula,  $(\text{Et}_3\text{NH})_3[\text{Cr}(\text{C}_6\text{F}_4\text{O}_2)_3]$ .

For the trianion in **1**,  $[\text{Cr}(\text{C}_6\text{F}_4\text{O}_2)_3]^{3-}$ , several valence tautomers such as  $[\text{Cr}^{\text{III}}(\text{F}_4\text{Cat})_3]^{3-}$ ,  $[\text{Cr}^{\text{II}}(\text{F}_4\text{Cat})_2(\text{F}_4\text{SQ})]^{3-}$ ,  $[\text{Cr}^{\text{I}}(\text{F}_4\text{Cat})(\text{F}_4\text{SQ})_2]^{3-}$ , or  $[\text{Cr}^{\text{0}}(\text{F}_4\text{SQ})_3]^{3-}$  ( $\text{F}_4\text{SQ} = \text{perfluorosemiquinonato}$ ) are conceivable, all of which differ with respect to their intramolecular charge distribution. The UV-vis-NIR spectrum of **1** in the solid state is shown in Figure 1b. Complex **1** shows a strong absorption peak at 220 nm with a shoulder at 280 nm, together with two weak absorption peaks at 420 and 590 nm. The two bands in the UV region can be assigned to  $\pi\text{-}\pi^*$  transitions of the  $\text{F}_4\text{Cat}^{2-}$  moieties,<sup>22</sup> while

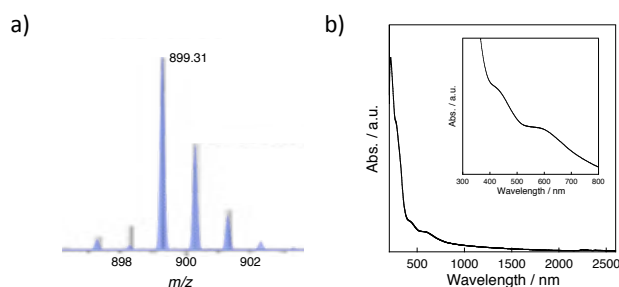


**Figure 1.** a) Positive-mode ESI-MS spectrum of **1** in MeCN (black lines) and the corresponding simulated spectrum (pale blue cones). b) Solid state (KBr pellet) UV-vis-NIR spectrum of **1**. The insert shows a magnification of the 300–800 nm region.

the two bands in the visible region are comparable to those of  $\text{K}_3[\text{Cr}^{\text{III}}(\text{Cat})_3]$  in water (425 and 592 nm) and were accordingly assigned to d-d transitions on the Cr(III) centre.<sup>21a</sup> Furthermore, the absence of charge transfer (CT;  $\text{Cr}^{\text{III}}/\text{SQ}^-$ ) bands in the visible region and intervalence CT (IVCT;  $\text{SQ}^- \leftarrow \text{Cat}^{2-}$ ) bands in the NIR region supported the absence of  $\text{F}_4\text{SQ}^-$  or  $\text{F}_4\text{Cat}^{2-}/\text{F}_4\text{SQ}^-$  mixed valence ligands. Based on these experimental results, the charge distribution of the three  $\text{C}_6\text{F}_4\text{O}_2$  ligands should be assigned as  $\text{F}_4\text{Cat}^{2-}$ , leading to the formulation of **1** as  $(\text{Et}_3\text{NH})_3[\text{Cr}^{\text{III}}(\text{F}_4\text{Cat})_3]$ .

### Solution UV-vis-NIR Spectra of **1**.

The UV-vis-NIR spectra of **1** in  $\text{CH}_2\text{Cl}_2$  and MeCN are shown in Figures 2a and 2b. In  $\text{CH}_2\text{Cl}_2$ , complex **1** exhibited three absorption peaks at 281 ( $13500 \text{ M}^{-1}\text{cm}^{-1}$ ), 441 (81), and 613 (73) nm. In MeCN, two absorption peaks at 285 ( $12500 \text{ M}^{-1}\text{cm}^{-1}$ ) and 600 (66) nm with one shoulder at 425 (88) nm were observed. The strong absorption bands at 281 and 285 nm in  $\text{CH}_2\text{Cl}_2$  and MeCN, respectively, should be assigned to  $\pi\text{-}\pi^*$  transitions on the aromatic ring of the  $\text{F}_4\text{Cat}^{2-}$ ,<sup>22</sup> while the weak absorption bands in the visible region should be ascribed to d-d transitions on the Cr(III) centre.<sup>21a</sup> In addition, the absence of absorption bands assignable to CT and IVCT bands suggests that complex **1** contains exhaustively reduced Cat ligands, in  $\text{CH}_2\text{Cl}_2$  and MeCN solution, as well as in the solid state.

### Redox Properties of **1**.

The cyclic voltammogram (CV) of **1** in  $\text{CH}_2\text{Cl}_2$  is shown in Figure 3a, and the corresponding data is summarized in Table 1. During an anodic scan, complex **1** showed three one-electron transfer waves at  $E_{1/2} = -0.12, 0.23, \text{ and } 0.53 \text{ V vs. Ag}/\text{Ag}^+$ . The first and second waves appear at more positive potentials than those of  $[\text{Cr}^{\text{III}}(\text{X}_4\text{SQ})_3]$  (for  $\text{X} = \text{Cl}$ :  $E_{1/2} = -0.28, 0.15, \text{ and } 0.53 \text{ V}$ ;<sup>13c</sup> for  $\text{X} = \text{Br}$ :  $E_{1/2} = -0.15, 0.11, \text{ and } 0.51 \text{ V}$ <sup>13b</sup>) measured under similar conditions. The redox potentials of these three-step processes might be closely related to not only the electron-withdrawing properties of the perhalogeno-groups but also to the electronic interactions between the three ligands. Potential gaps, *i.e.*,  $\Delta E^a = E_{1/2}^2 - E_{1/2}^1$  and  $\Delta E^b = E_{1/2}^3 - E_{1/2}^2$ , of 0.43 and 0.38 V for  $[\text{Cr}^{\text{III}}(\text{Cl}_4\text{SQ})_3]$ , as well as 0.26 and 0.40 V for  $[\text{Cr}^{\text{III}}(\text{Br}_4\text{SQ})_3]$ , respectively, were estimated.

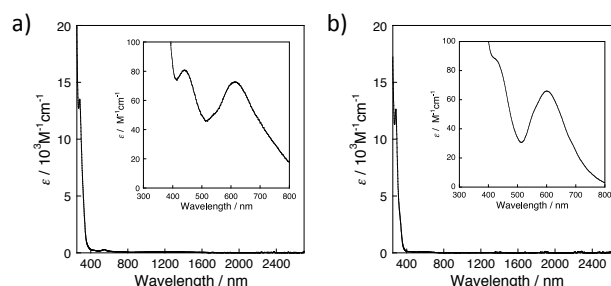


**Figure 2.** UV-vis-NIR spectra of **1** ( $5 \times 10^{-4} \text{ M}$ ) in a)  $\text{CH}_2\text{Cl}_2$  and b) MeCN under an atmosphere of  $\text{N}_2$ . The insets show a magnification of the 300–800 nm region.

**Table 1.** Electrochemical data for **1** in CH<sub>2</sub>Cl<sub>2</sub> and MeCN at 20 mV·s<sup>-1</sup> (V vs. Ag/Ag<sup>+</sup>)

Solvent	$E_{pa}^1$	$E_{pc}^1$	$E_{1/2}^1$ ( $\Delta E^1$ )	$E_{pa}^2$	$E_{pc}^2$	$E_{1/2}^2$ ( $\Delta E^2$ )	$E_{pa}^3$	$E_{pc}^3$	$E_{1/2}^3$ ( $\Delta E^3$ )
CH <sub>2</sub> Cl <sub>2</sub>	-0.06	-0.17	-0.12 (0.11)	0.29	0.16	0.23 (0.13)	0.58	0.48	0.53 (0.10)
MeCN	-0.16	-0.25	-0.21 (0.09)	0.11	0.04	0.08 (0.07)	0.55	0.45	0.50 (0.10)

The corresponding  $\Delta E^a$  and  $\Delta E^b$  values for [Cr<sup>III</sup>(Cl<sub>4</sub>SQ)<sub>3</sub>], as well as the  $\Delta E^b$  value for [Cr<sup>III</sup>(Br<sub>4</sub>SQ)<sub>3</sub>] are larger than those of **1** ( $\Delta E^a = 0.35$  and  $\Delta E^b = 0.30$  V). Conversely, [Cr<sup>III</sup>(Br<sub>4</sub>SQ)<sub>3</sub>] exhibited a comparatively small  $\Delta E^a$  value, which is indicative of two-electron transfer reactions occurring in between 0.26 V. In the case of **1**, the  $\Delta E^a$  and  $\Delta E^b$  values are moderate, and the average of the three potential values (0.21 V vs. Ag/Ag<sup>+</sup>) is more positive than that of [Cr<sup>III</sup>(X<sub>4</sub>SQ)<sub>3</sub>] (for X = Cl: 0.13 V; for X = Br: 0.16 V). The observed strong electron-accepting ability should be attributed to the strong electron-withdrawing effect of the perfluoro-groups. CV experiments at different scan rates (10, 20, 50, 100, 200, and 400 mV·s<sup>-1</sup>) demonstrated that  $\Delta E^1$ ,  $\Delta E^2$ , and  $\Delta E^3$  ( $\Delta E = \Delta E_{pa} - \Delta E_{pc}$ ) values decrease with decreasing scan rates as shown in Figures S2a and S3. Therefore, these three redox waves can be assigned to quasi-reversible processes.

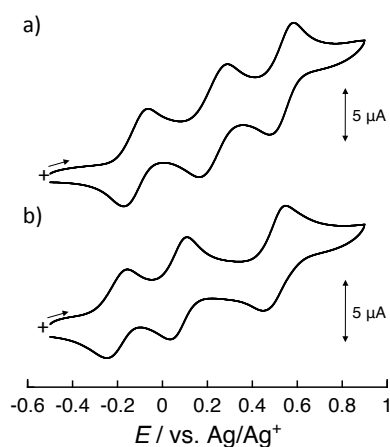
In non-polar solvents such as CH<sub>2</sub>Cl<sub>2</sub>, complexes of the type [Cr<sup>III</sup>(X<sub>4</sub>Cat)<sub>x</sub>(X<sub>4</sub>SQ)<sub>3-x</sub>]<sup>x-</sup> (X = Cl and Br; x = 0, 1, 2) are known to be stable, whereas [Cr<sup>III</sup>(Cl<sub>4</sub>SQ)<sub>3</sub>] exhibits the ligand substitution reaction in highly polar solvents such as MeCN, resulting in the formation of [Cr<sup>III</sup>(Cl<sub>4</sub>Cat)(Cl<sub>4</sub>SQ)(MeCN)<sub>2</sub>].<sup>23</sup>

Despite the previously reported instability of [Cr<sup>III</sup>(Cl<sub>4</sub>SQ)<sub>3</sub>] in MeCN,<sup>23</sup> a MeCN solution of **1** exhibited three redox waves at  $E_{1/2} = -0.21$ , 0.08, and 0.50 V, all of which are very similar to those in CH<sub>2</sub>Cl<sub>2</sub> (Figure 3b). These waves appear at more negative potentials ( $E_{1/2}(\text{MeCN}) - E_{1/2}(\text{CH}_2\text{Cl}_2) = -0.09$ ,  $-0.20$ , and  $-0.03$  V) relative to those in CH<sub>2</sub>Cl<sub>2</sub>. The observed potential shifts should accordingly relate to differences in solvent polarity between CH<sub>2</sub>Cl<sub>2</sub> and MeCN.<sup>24</sup> If the ligands act

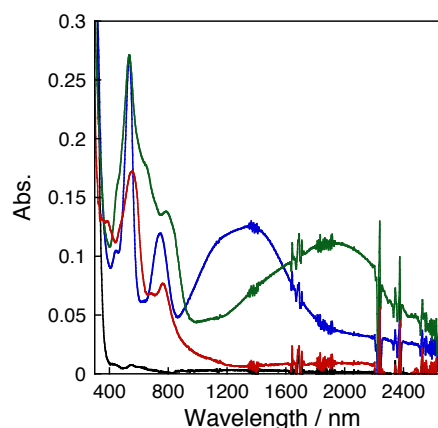
as redox-centres in these reactions (for the assignment of redox-sites, see the next section), the one- and two-electron oxidized species of **1**, *i.e.* [Cr<sup>III</sup>(F<sub>4</sub>Cat)<sub>2</sub>(F<sub>4</sub>SQ)]<sup>2-</sup> and [Cr<sup>III</sup>(F<sub>4</sub>Cat)(F<sub>4</sub>SQ)<sub>2</sub>]<sup>-</sup>, should possess a dipole moment. This dipole moment should arise from the asymmetric, mixed valence charge distribution in the ligands, which is dissimilar to **1** with homoleptic ligands. Following this notion, the high solvent polarity of MeCN may be able to influence to the solvation energy of the redox-isomers of **1**.<sup>25</sup> On the basis of variable scan rate experiments in MeCN, the three waves were assigned to quasi-reversible processes in the 20-400 mV·s<sup>-1</sup> range (Figures S2b and S3). Moreover, the voltammogram for **1** showed remarkable reproducibility upon repeating the cyclic scans at 20 mV·s<sup>-1</sup> (Figure S4). Therefore, complex **1** and its one-, two-, and three-electron oxidized species can be expected to kinetically maintain their structures in MeCN solution.

#### Assignment of Redox Sites in **1**.

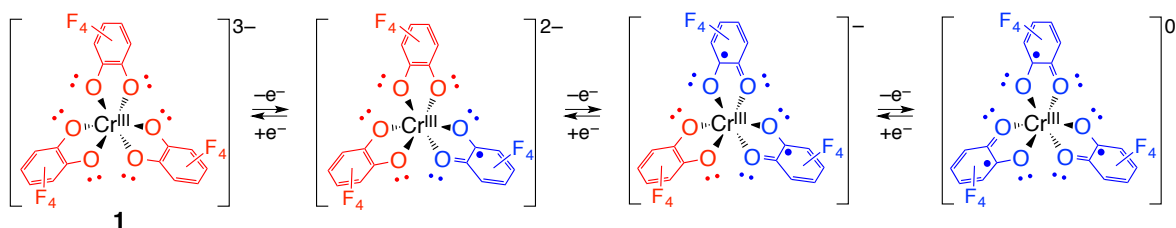
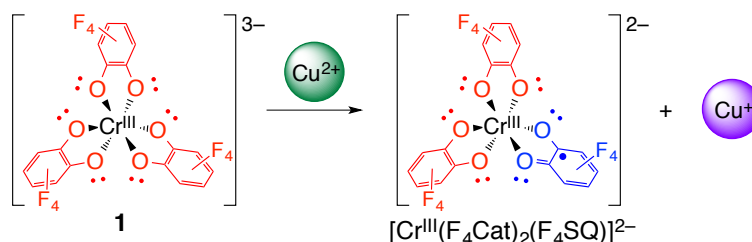
The assignments of redox sites in metal complexes, bearing both redox-active metals and ligands, should be undertaken carefully. For example, [Cr<sup>III</sup>(X<sub>4</sub>SQ)<sub>3</sub>] (X = Cl and Br), accepts electrons on the ligand sites to form [Cr<sup>III</sup>(X<sub>4</sub>Cat)(X<sub>4</sub>SQ)<sub>2</sub>]<sup>-</sup>, [Cr<sup>III</sup>(X<sub>4</sub>Cat)<sub>2</sub>(X<sub>4</sub>SQ)]<sup>2-</sup>, and [Cr<sup>III</sup>(X<sub>4</sub>Cat)<sub>3</sub>]<sup>3-</sup>.<sup>13</sup> In CH<sub>2</sub>Cl<sub>2</sub>, the one-electron reduced [Cr<sup>III</sup>(X<sub>4</sub>Cat)(X<sub>4</sub>SQ)<sub>2</sub>]<sup>-</sup> shows CT and IVCT bands at 546 (CT) and 2180 (IVCT) nm for X = Cl, and at 546 (CT) and 2200 nm (IVCT) for X = Br. The corresponding bands of the two-electron reduced [Cr<sup>III</sup>(X<sub>4</sub>Cat)<sub>2</sub>(X<sub>4</sub>SQ)]<sup>2-</sup> appear at 540 (CT) and 1680 nm (IVCT) with a shoulder at 1200 nm for X



**Figure 3.** CVs of **1** (1 mM) in a) CH<sub>2</sub>Cl<sub>2</sub> and b) MeCN: recorded at 20 mV·s<sup>-1</sup> under an atmosphere of Ar using *n*-Bu<sub>4</sub>NPF<sub>6</sub> (0.1 M).



**Figure 4.** UV-vis-NIR spectra of **1** ( $5 \times 10^{-4}$  M) in CH<sub>2</sub>Cl<sub>2</sub> at rest potential (black line),  $-0.05$  V (blue line),  $0.35$  V (green line), and  $0.9$  V vs. Ag/Ag<sup>+</sup> (red line) under an atmosphere of Ar using *n*-Bu<sub>4</sub>NPF<sub>6</sub> (0.1 M).

Scheme 2. Scheme for the redox processes of **1**Scheme 3. Redox reaction scheme between **1** and  $\text{Cu}^{2+}$ 

= Cl, and at 540 (CT) and 1660 nm (IVCT) with a shoulder at 1200 nm for  $X = \text{Br}$ .<sup>13a</sup>

The UV-vis-NIR spectra of **1** during bulk electrolysis in  $\text{CH}_2\text{Cl}_2$  are shown in Figure 4. Strong absorption bands appeared in the visible and NIR regions (446, 536, 630sh., 750, 1140sh., and 1380 nm) during the first oxidation at  $-0.05$  V vs.  $\text{Ag}/\text{Ag}^+$  (blue line). The characteristic bands at 536, 1140sh., and 1380 nm thereby resemble those of  $[\text{Cr}^{\text{III}}(\text{X}_4\text{Cat})_2(\text{X}_4\text{SQ})]^{2-}$  ( $X = \text{Cl}$  and  $\text{Br}$ ).<sup>13a</sup> Accordingly, the electrochemically generated one-electron oxidized species of **1** should be assigned the empirical formula  $[\text{Cr}^{\text{III}}(\text{F}_4\text{Cat})_2(\text{F}_4\text{SQ})]^{2-}$ . The bands observed at 536 and 1380 with 1140sh. nm were assigned to CT ( $\text{Cr}^{\text{III}}/\text{F}_4\text{SQ}^-$ ) and IVCT ( $\text{F}_4\text{SQ}^- - \text{F}_4\text{Cat}^{2-}$ ) bands, respectively. The second oxidation at 0.35 V (green line) exhibited an unchanged CT band at 536 nm and a red-shifted IVCT band around 1950 nm. These characteristics are very similar to those of  $[\text{Cr}^{\text{III}}(\text{X}_4\text{Cat})(\text{X}_4\text{SQ})_2]^-$  ( $X = \text{Cl}$  and  $\text{Br}$ ),<sup>13a</sup> and accordingly, the electrochemically generated two-electron oxidized species of **1** should be assigned the empirical formula  $[\text{Cr}^{\text{III}}(\text{F}_4\text{Cat})(\text{F}_4\text{SQ})_2]^-$ . Upon further oxidation at 0.9 V (red line), the CT band remained at 554 nm, whereas a strong absorption band assignable to IVCT could not be observed, similar to the case of  $[\text{Cr}^{\text{III}}(\text{X}_4\text{SQ})_3]$ .<sup>13a</sup> It should therefore be reasonable to assume

that the valence states of the ligands in the three-electron oxidized species of **1** became equivalent to the  $\text{F}_4\text{SQ}^-$  state, leading to the formulation of  $[\text{Cr}^{\text{III}}(\text{F}_4\text{SQ})_3]$ . Considering all these spectral results, the three oxidation steps of **1** can be assigned to three ligand-centred one-electron transfer steps, consecutively generating  $[\text{Cr}^{\text{III}}(\text{F}_4\text{Cat})_2(\text{F}_4\text{SQ})]^{2-}$ ,  $[\text{Cr}^{\text{III}}(\text{F}_4\text{Cat})(\text{F}_4\text{SQ})_2]^-$ , and  $[\text{Cr}^{\text{III}}(\text{F}_4\text{SQ})_3]$  as shown in Scheme 2.

#### Redox Reaction between **1** and $\text{Cu}^{2+}$ Ion.

As previously discussed, complex **1** shows well-defined three-step redox behaviour in MeCN. As MeCN is a good solvent not only for **1**, but also for several metal perchlorate salts, titration experiments were carried out in this solvent. The addition of one equivalent of  $\text{Cu}(\text{ClO}_4)_2 \cdot 6\text{H}_2\text{O}$  to a MeCN solution of **1**, resulted in the emergence of new bands at 443, 536, 629, 763, 1230sh., and 1540 nm as shown in Figure 5a. The resulting spectrum is thus identical to that of the electrochemically generated one-electron oxidized form of **1**,  $[\text{Cr}^{\text{III}}(\text{F}_4\text{Cat})_2(\text{F}_4\text{SQ})]^{2-}$  (black line; Figure 5b, and Figure S5). A similar spectrum is also obtained from the addition of  $[\text{Cu}(\text{MeCN})_4]\text{PF}_6$  to an electrochemically generated solution of  $[\text{Cr}^{\text{III}}(\text{F}_4\text{Cat})_2(\text{F}_4\text{SQ})]^{2-}$  in MeCN (red line; Figure 5b). It was thus confirmed that  $\text{Cu}^{\text{II}}(\text{ClO}_4)_2 \cdot 6\text{H}_2\text{O}$  shows a  $\text{Cu}^+/\text{Cu}^{2+}$  redox couple at  $E_{1/2} = 0.75$  V vs.  $\text{Ag}/\text{Ag}^+$  in MeCN (Figure S6). The potential of the  $\text{Cu}^+/\text{Cu}^{2+}$  couple is higher than that of  $[\text{Cr}^{\text{III}}(\text{F}_4\text{Cat})_3]^{3-}/[\text{Cr}^{\text{III}}(\text{F}_4\text{Cat})_2(\text{F}_4\text{SQ})]^{2-}$  ( $E_{1/2}^1 = -0.21$  V). Accordingly, complex **1** should be oxidized by  $\text{Cu}^{2+}$  to give  $[\text{Cr}^{\text{III}}(\text{F}_4\text{Cat})_2(\text{F}_4\text{SQ})]^{2-}$  and  $\text{Cu}^+$  (Scheme 3). The close resemblance of the spectra of this mixture with electrochemically generated  $[\text{Cr}^{\text{III}}(\text{F}_4\text{Cat})_2(\text{F}_4\text{SQ})]^{2-}$  independent of the absence or presence of  $\text{Cu}^+$ , is thereby indicative of a negligible interaction between  $[\text{Cr}^{\text{III}}(\text{F}_4\text{Cat})_2(\text{F}_4\text{SQ})]^{2-}$  and  $\text{Cu}^+$ . In general,  $\text{Cu}^+$  is considered a soft metal ion,<sup>26</sup> and the interactions between  $\text{Cu}^+$  and the hard lone pairs on the oxygen atoms of the  $\text{F}_4\text{Cat}^{2-}$  moieties in  $[\text{Cr}^{\text{III}}(\text{F}_4\text{Cat})_2(\text{F}_4\text{SQ})]^{2-}$  should be minimal (*vide infra*).

#### Interaction of **1** with Guest Metal Ions.

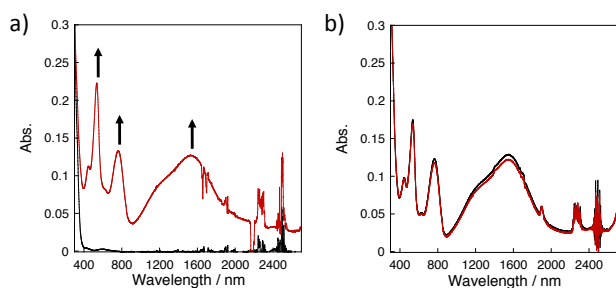


**Figure 5.** a) Changes of the UV-vis-NIR spectrum of **1** ( $5 \times 10^{-5}$  M, black line) upon addition of one equivalent of  $\text{Cu}(\text{ClO}_4)_2 \cdot 6\text{H}_2\text{O}$  (red line) in MeCN. b) UV-vis-NIR spectra of **1** ( $5 \times 10^{-5}$  M) electrolysed at  $-0.1$  V vs.  $\text{Ag}/\text{Ag}^+$  (black line) and upon addition of one equivalent of  $[\text{Cu}(\text{MeCN})_4]\text{PF}_6$  (red line) under an atmosphere of  $\text{N}_2$  using  $n\text{-Bu}_4\text{NPF}_6$  ( $1 \times 10^{-2}$  M).

Figure 6 shows the UV-vis-NIR spectral changes of **1** upon addition of 0.5 and 1 equivalent of metal perchlorates, *i.e.*, LiClO<sub>4</sub> or M(ClO<sub>4</sub>)<sub>2</sub>·6H<sub>2</sub>O (M = Mn, Fe, Co, and Zn) in MeCN. The addition of Li<sup>+</sup> to the MeCN solution of **1** led to a decrease of the absorbance at 285 nm, whereas no change was observed in the visible and NIR regions (Figure 6a). The spectral changes at 285 nm ( $\pi$ - $\pi^*$  transition) suggest an interaction between **1** and Li<sup>+</sup>, indicating a modulation of the  $\pi$ - $\pi^*$  transition on the F<sub>4</sub>Cat<sup>2-</sup> moieties. Similar spectral changes were observed for [Na(thf)<sub>3</sub>{*fac*-Mo<sup>V</sup>(Mp)<sub>3</sub>}] and [Mn<sup>II</sup>(H<sub>2</sub>O)(MeOH){*fac*-Mo<sup>V</sup>(Mp)<sub>3</sub>}]<sub>2</sub> in *o*-dichlorobenzene (Figure S7).<sup>17</sup> The absorbance of the  $\pi$ - $\pi^*$  band in the Mp<sup>2-</sup> moieties decreases as a result of the binding interactions with Na<sup>+</sup> and Mn<sup>2+</sup> *via* the lone pairs on the coordinating oxygen atoms. Therefore, it is reasonable to conclude that complex **1** should interact with Li<sup>+</sup> in a similar manner *via* the lone pairs on the coordinating oxygen atom(s) of the F<sub>4</sub>Cat<sup>2-</sup> moieties. As shown in Figure 7a, a Job's plot obtained from a continuous variation method, monitoring the absorbance at 285 nm, shows a peak top at a mole fraction ( $[\text{Li}^+]/([\text{Li}^+]+[\mathbf{1}]) = 0.5$ ,<sup>27</sup> indicating a one-to-one interaction between **1** and Li<sup>+</sup>.

Similarly with this case, addition of Mn<sup>2+</sup>, Fe<sup>2+</sup>, Co<sup>2+</sup>, or Zn<sup>2+</sup> induced similar spectral changes as shown in Figures 6b-6e. In

contrast to the case of Cu<sup>2+</sup>, these spectral features indicate that complex **1** interacts with these guest metal ions without changing its original oxidation state and charge distribution. Each Job's plot exhibits a peak at a mole fraction of 0.5 (Figures 7b-7e). Accordingly, complex **1** should interact with Mn<sup>2+</sup>, Fe<sup>2+</sup>, Co<sup>2+</sup>, and Zn<sup>2+</sup> in a one-to-one ratio, similarly to the case of Li<sup>+</sup>. The plots also indicate that further interaction with one or two more guest metal ions did not occur in MeCN. The Coulomb interactions between the one-to-one complexes and further guest metal ions might be weaker than that between **1** and guest metal ion, because the effective anionic charge of the RML is decreased by the interaction with the first guest metal ion.

In order to quantitatively determine the affinity between **1** and the guest metal ions, further UV-vis titration experiments were carried out as shown in Figure 8. The binding constant (*K*) values can be estimated by applying eq. 1 in a region that contains no absorption bands of the guest molecule:<sup>28</sup>

$$\Delta A_{\text{obs}} = \frac{b\Delta\epsilon}{2K} (X - \{X^2 - 4K^2[H]_0[G]_0\}^{1/2}) \quad \text{eq. 1}$$

$$X = 1 + K[H]_0 + K[G]_0$$

where [H]<sub>0</sub>, [G]<sub>0</sub>,  $\Delta A_{\text{obs}}$ , *b*, and  $\Delta\epsilon$  refer to the initial

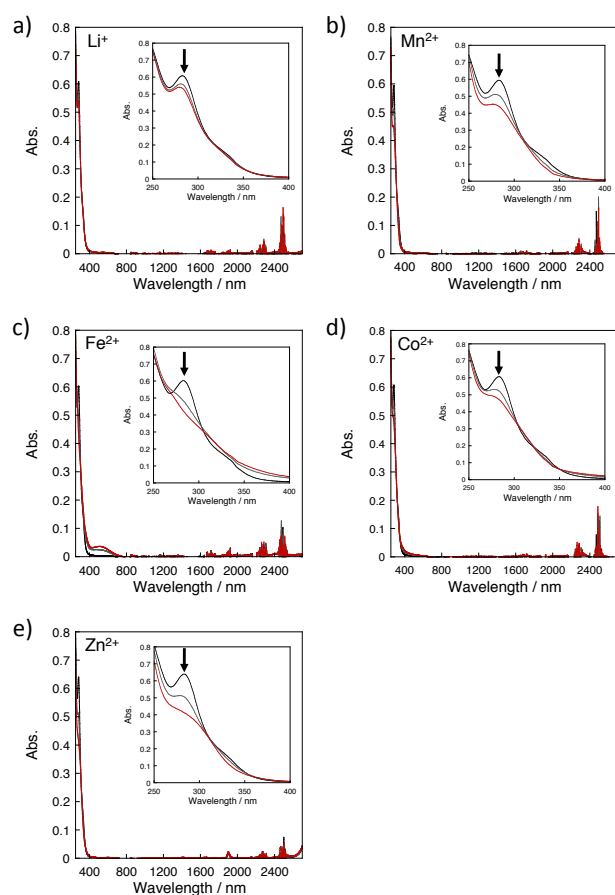


**Figure 6.** Changes of the UV-vis-NIR spectrum of **1** ( $5 \times 10^{-5}$  M, black line) in MeCN upon addition of 0.5 (grey line) and one equivalent (red line) of a) LiClO<sub>4</sub>, b) Mn(ClO<sub>4</sub>)<sub>2</sub>·6H<sub>2</sub>O, c) Fe(ClO<sub>4</sub>)<sub>2</sub>·6H<sub>2</sub>O, d) Co(ClO<sub>4</sub>)<sub>2</sub>·6H<sub>2</sub>O, or e) Zn(ClO<sub>4</sub>)<sub>2</sub>·6H<sub>2</sub>O. The insets show a magnification of the 250-400 nm region.

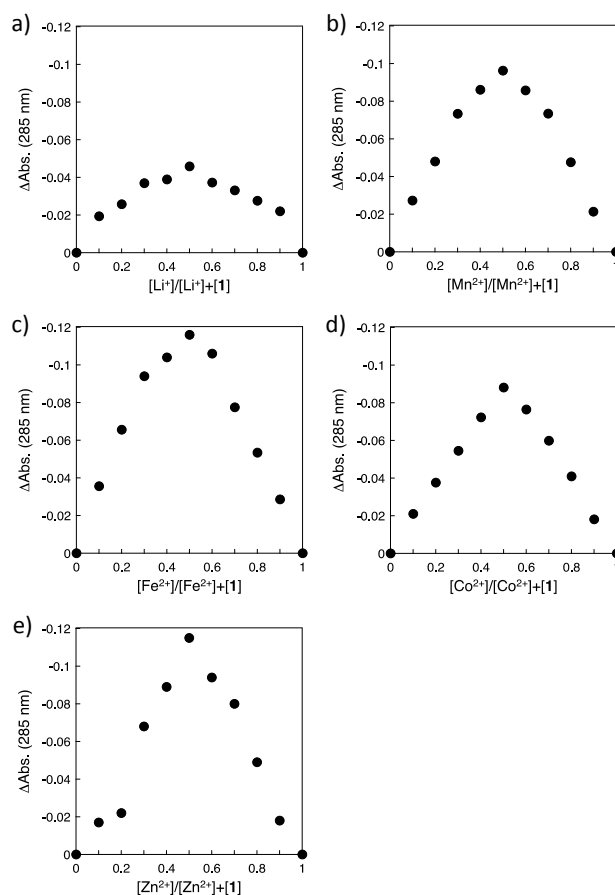


**Figure 7.** Job's plots for **1** upon addition of a) LiClO<sub>4</sub>, b) Mn(ClO<sub>4</sub>)<sub>2</sub>·6H<sub>2</sub>O, c) Fe(ClO<sub>4</sub>)<sub>2</sub>·6H<sub>2</sub>O, d) Co(ClO<sub>4</sub>)<sub>2</sub>·6H<sub>2</sub>O, or e) Zn(ClO<sub>4</sub>)<sub>2</sub>·6H<sub>2</sub>O, monitored by differential absorbances at 285 nm.

concentration of the host, the initial concentration of the guest, the observed differential absorbance of the mixture and  $[H]_0$ , the optical path length, and the differential molar extinction coefficient of the host-guest complex and the host, respectively.

The  $K$  value for  $Li^+$  was estimated to be  $3.7 (\pm 0.3) \times 10^4 M^{-1}$ , while those for  $Mn^{2+}$ ,  $Fe^{2+}$ ,  $Co^{2+}$ , and  $Zn^{2+}$  were estimated to be  $1.5 (\pm 0.2) \times 10^5$ ,  $2.2 (\pm 0.4) \times 10^5$ ,  $1.9 (\pm 0.2) \times 10^5$ , and  $3.8 (\pm 0.4) \times 10^5 M^{-1}$ , respectively. These results suggest that the interaction between divalent guest metal ions and **1** is by one order of magnitude higher than that of monovalent cations such as  $Li^+$ . Nabeshima *et al.* have reported that the neutral

ML  $[Al^{III}(\text{dipyrrin})(H_2O)_2]$  (dipyrrin =  $C_{27}H_{17}N_2O_2$ ) binds to  $ZnCl_2$  in toluene/MeOH (99/1) in a one-to-one ratio *via* the lone pairs of two oxygen atoms of the dipyrin, and a  $K$  value was of  $6.1 (\pm 1.3) \times 10^6 M^{-1}$  was reported.<sup>29</sup> This value suggests that not only electrostatic (Coulombic), but also covalent interactions between the ML and guest metal ion play an important role.

In order to obtain further information about the interactions between **1** and guest metal ions, ESI-MS measurements of MeCN solutions containing **1** and one equivalent of metal perchlorates were carried out. As shown in Figures 9 and S8-S12, these solutions exhibited peaks at  $m/z = 599.92$  ( $Li^+$ ),

**Scheme 4.** Binding interaction between **1** and guest metal ions

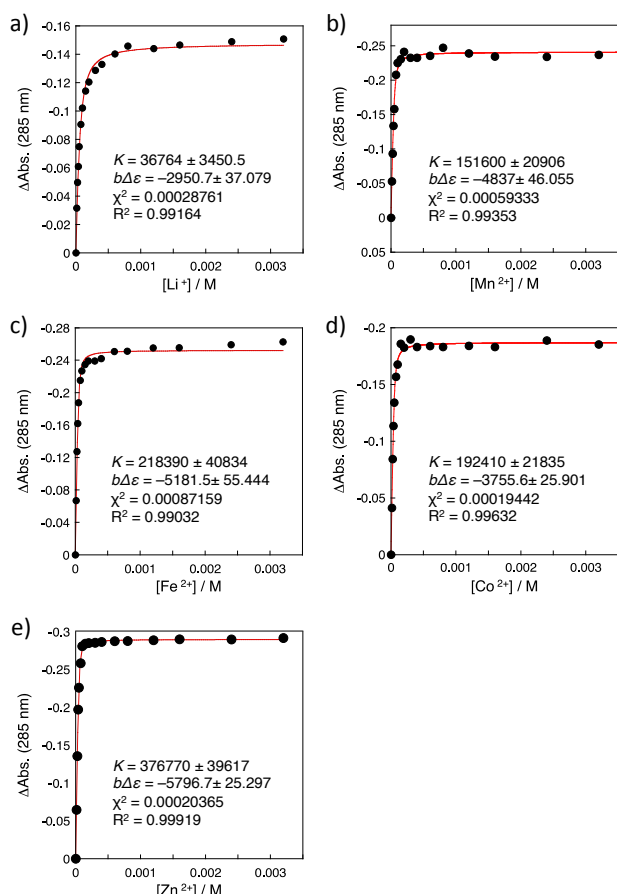
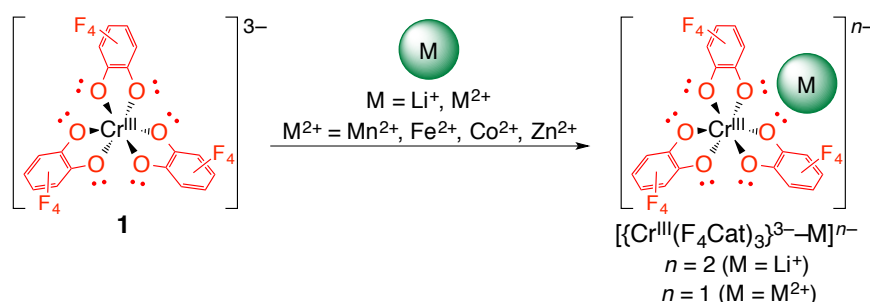


**Figure 8.** Differential absorbance profiles (285 nm) and fitting curves (red line) for mixtures of **1** ( $5 \times 10^{-5} M$ ) and 0, 1.25, 2.5, 3.75, 5, 7.5, 10, 15, 20, 30, 40, 60, 80, 120, 160, 240, and  $320 \times 10^{-5} M$  of a)  $LiClO_4$ , b)  $Mn(ClO_4)_2 \cdot 6H_2O$ , c)  $Fe(ClO_4)_2 \cdot 6H_2O$ , d)  $Co(ClO_4)_2 \cdot 6H_2O$ , and e)  $Zn(ClO_4)_2 \cdot 6H_2O$ ; monitored in MeCN solution using a 1.0 cm cell at room temperature.

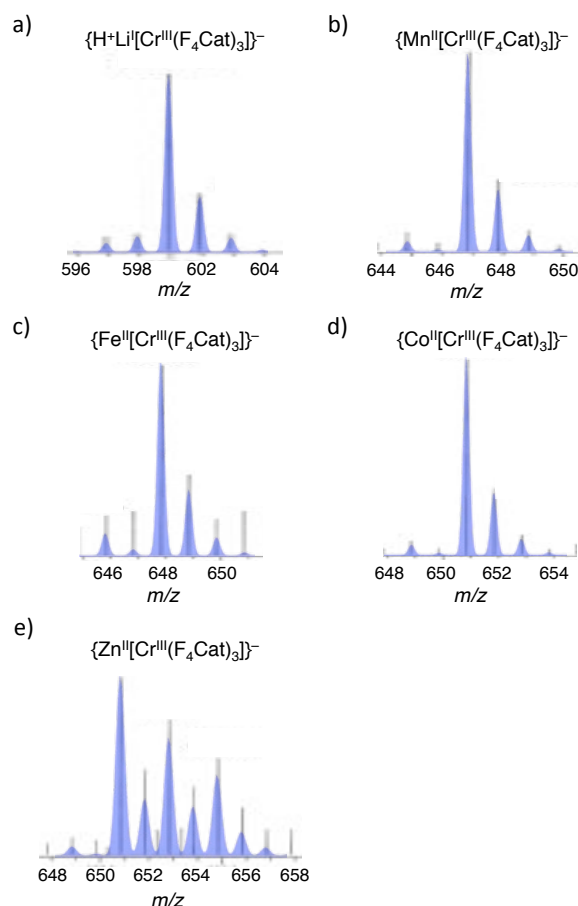


**Figure 9.** Negative-mode ESI-MS spectra in the  $m/z = 590-660$  region of MeCN solutions containing **1** and one equivalent of a)  $LiClO_4$ , b)  $Mn(ClO_4)_2 \cdot 6H_2O$ , c)  $Fe(ClO_4)_2 \cdot 6H_2O$ , d)  $Co(ClO_4)_2 \cdot 6H_2O$ , and e)  $Zn(ClO_4)_2 \cdot 6H_2O$ . Pale-blue cones represent the corresponding simulated spectra.

646.83 (Mn<sup>2+</sup>), 647.83 (Fe<sup>2+</sup>), 650.83 (Co<sup>2+</sup>), and 655.83 (Zn<sup>2+</sup>). These values are consistent with the exact mass of {H<sup>+</sup>Li<sup>+</sup>[Cr<sup>III</sup>(F<sub>4</sub>Cat)<sub>3</sub>]}<sup>-</sup> (599.91), {Mn<sup>II</sup>[Cr<sup>III</sup>(F<sub>4</sub>Cat)<sub>3</sub>]}<sup>-</sup> (646.83), {Fe<sup>II</sup>[Cr<sup>III</sup>(F<sub>4</sub>Cat)<sub>3</sub>]}<sup>-</sup> (647.83), {Co<sup>II</sup>[Cr<sup>III</sup>(F<sub>4</sub>Cat)<sub>3</sub>]}<sup>-</sup> (650.82), and {Zn<sup>II</sup>[Cr<sup>III</sup>(F<sub>4</sub>Cat)<sub>3</sub>]}<sup>-</sup> (655.82), whereby each isotopic composition was found to be in agreement with simulated patterns. Therefore, these results support the formation of one-to-one complexes between **1** and guest metal ions in MeCN (Scheme 4).

### Redox Properties of **1** with Guest Metal Ions

Figure 10 shows the CVs of **1** upon addition of one equivalent of guest metal ions in MeCN, and the electrochemical data is summarized in Table 2. As shown in the figure, addition of the guest metal ions led to variations in all of the voltammograms. Addition of Li<sup>+</sup> resulted in a slight positive shift of the first oxidation peak by 0.08 V relative to that of parent **1**, while maintaining three well-defined redox couples (Figure 10b). The observed positive shift indicates an interaction between Li<sup>+</sup> and **1**,<sup>17</sup> which should decrease the electron density on the [Cr<sup>III</sup>(F<sub>4</sub>Cat)<sub>3</sub>]<sup>3-</sup> moiety. On the other hand, the second and third oxidation peaks appeared at potentials similar to those of **1**. Based on these results, it is suggested that Li<sup>+</sup> binds to **1**, while it exerted negligible impact on the electronic environment of the oxidized species. Among the four divalent metal ions used, Mn<sup>2+</sup> and Co<sup>2+</sup> led to a disappearance of the first oxidation peak observed at -0.16 V for **1** (Figures 10c and 10e). Instead, the oxidation peaks appeared at significantly positive-shifted potentials at ca. 0.1 V. Finally, addition of Fe<sup>2+</sup> or Zn<sup>2+</sup> afforded the voltammograms with weak anodic currents at ca. 0.1 V, and subsequent oxidation peaks (Figures 10d and 10f). The electrochemical data thus support interactions between **1** and the divalent metal ions not only at rest potentials, which is revealed by the titration experiments, but also at more positive potentials.

In order to reveal the electrochemically generated species in the presence of guest metal ions, spectroelectrochemical measurements were carried out. First, Figure 11a shows a spectrum of a MeCN solution containing **1** and one equivalent of Li<sup>+</sup> electrolyzed at -0.08 V vs. Ag/Ag<sup>+</sup> for 36 min (black line) together with that of **1** electrolyzed at -0.10 V (blue line). The

electrolysis of **1** with Li<sup>+</sup> gave absorption peaks at 445, 535, 626, 764, 1230sh., and 1540 nm, which are identical with those of the electrochemically generated [Cr<sup>III</sup>(F<sub>4</sub>Cat)<sub>2</sub>(F<sub>4</sub>SQ)]<sup>2-</sup>. A similar spectrum can be also obtained by adding one equivalent of Li<sup>+</sup> to a solution of the electrochemically generated [Cr<sup>III</sup>(F<sub>4</sub>Cat)<sub>2</sub>(F<sub>4</sub>SQ)]<sup>2-</sup> (Figure S13a). Accordingly, the one-electron oxidation should proceed on the ligand moiety of [Cr<sup>III</sup>(F<sub>4</sub>Cat)<sub>3</sub>]<sup>3-</sup>-Li<sup>+</sup><sup>2-</sup> similar to the case of **1**. Although information on the interaction between [Cr<sup>III</sup>(F<sub>4</sub>Cat)<sub>2</sub>(F<sub>4</sub>SQ)]<sup>2-</sup> and Li<sup>+</sup> is not available at this stage, the one-electron oxidation process is confirmed to be sufficiently reversible (eq. 2, Figures S14a and S14b).

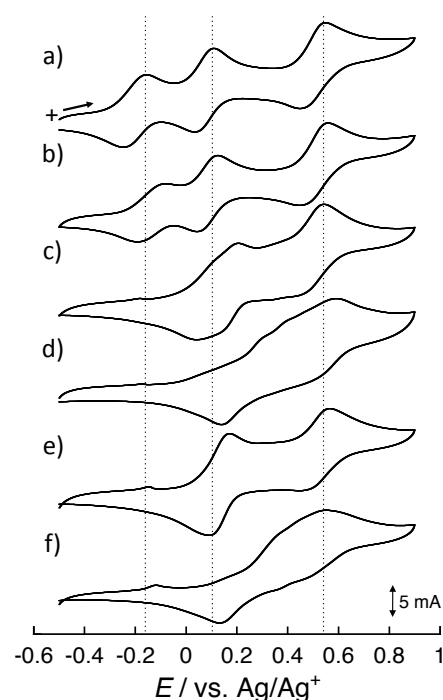


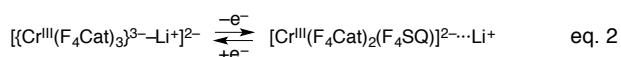
**Figure 10.** a) CVs of **1** (1 mM) in MeCN upon addition of one equivalent of b) LiClO<sub>4</sub>, c) Mn(ClO<sub>4</sub>)<sub>2</sub>·6H<sub>2</sub>O, d) Fe(ClO<sub>4</sub>)<sub>2</sub>·6H<sub>2</sub>O, e) Co(ClO<sub>4</sub>)<sub>2</sub>·6H<sub>2</sub>O, or f) Zn(ClO<sub>4</sub>)<sub>2</sub>·6H<sub>2</sub>O at 20 mV·s<sup>-1</sup> under an atmosphere of Ar using *n*-Bu<sub>4</sub>NPF<sub>6</sub> (0.1 M).

**Table 2.** Electrochemical data for **1** and for **1** in the presence of M(ClO<sub>4</sub>)<sub>n</sub> (n = 1-2) in MeCN at 20 mV·s<sup>-1</sup>

	(V vs. Ag/Ag <sup>+</sup> )									
	$E_{pa}^1$	$E_{pc}^1$	$E_{1/2}^1$ ( $\Delta E^1$ )	$E_{pa}^2$	$E_{pc}^2$	$E_{1/2}^2$ ( $\Delta E^2$ )	$E_{pa}^3$	$E_{pc}^3$	$E_{1/2}^3$ ( $\Delta E^3$ )	$E_{pa}^4$
<b>1</b>	-0.16	-0.25	-0.21	0.11	0.04	0.08	0.55	0.45	0.50	
<b>1</b> + Li <sup>+</sup>	-0.08	-0.18	-0.13 (0.10)	0.12	0.05	0.09 (0.07)	0.56	0.46	0.51 (0.10)	
<b>1</b> + Mn <sup>2+</sup>	0.10 <sup>a</sup>	0.04	0.07 (0.06)	0.21	0.15 <sup>a</sup>	0.18 (0.06)	0.55	0.45	0.50 (0.10)	
<b>1</b> + Fe <sup>2+</sup>	0.10 <sup>a</sup>	0.14		0.30 <sup>a</sup>	0.51 <sup>a</sup>		0.40 <sup>a</sup>			0.59
<b>1</b> + Co <sup>2+</sup>	0.17 <sup>b</sup>	0.09 <sup>b</sup>	0.13 (0.08)	0.57	0.46	0.52 (0.11)				
<b>1</b> + Zn <sup>2+</sup>	0.17 <sup>a</sup>	0.14		0.37 <sup>a</sup>	0.37 <sup>a</sup>		0.46 <sup>a</sup>	0.48 <sup>a</sup>		0.55

<sup>a</sup>Shoulder peak

<sup>b</sup>Two-electron transfer process



Further oxidation at 0.35 V for 6 min gave a transient spectrum showing characteristic features of the two-electron oxidized species  $[\text{Cr}^{\text{III}}(\text{F}_4\text{Cat})(\text{F}_4\text{SQ})_2]^-$  (Figure S14c). After these initial changes relative to the original spectrum, the spectrum exhibited further variations and afforded a different spectrum. This is due to instability of the two-electron oxidized species in MeCN (Figures S5d and S14d), and a ligand exchange reaction can be suspected (Scheme S1).<sup>23</sup>

In contrast, electrolysis of a solution of **1** in the presence of

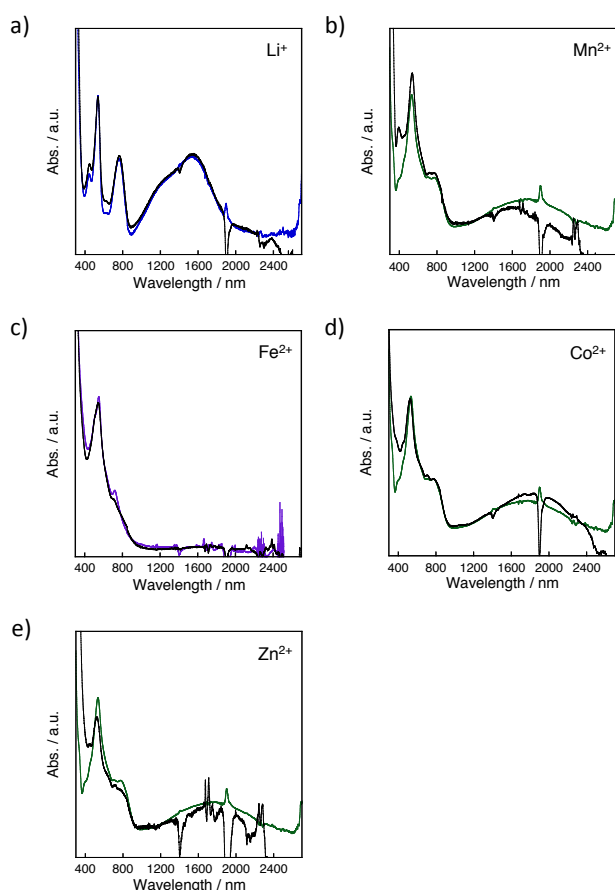
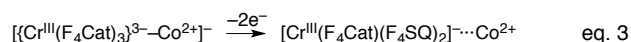
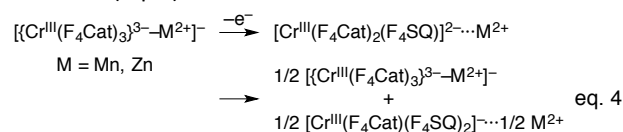


**Figure 11.** The UV-vis-NIR spectra of **1** ( $5 \times 10^{-4}$  M) with 1 eq. of a)  $\text{LiClO}_4$  electrolyzed at  $-0.08$  V vs.  $\text{Ag}/\text{Ag}^+$  for 36 min (black line) and electrochemically generated  $[\text{Cr}^{\text{III}}(\text{F}_4\text{Cat})_2(\text{F}_4\text{SQ})_2]^{2-}$  prepared from **1** ( $5 \times 10^{-4}$  M) electrolyzed at  $-0.1$  V for 21 min (blue line), b)  $\text{Mn}(\text{ClO}_4)_2 \cdot 6\text{H}_2\text{O}$  electrolyzed at 0.12 V for 6 min (black line) and electrochemically generated  $[\text{Cr}^{\text{III}}(\text{F}_4\text{Cat})(\text{F}_4\text{SQ})_2]^-$  prepared from **1** ( $5 \times 10^{-4}$  M) electrolyzed at 0.35 V for 21 min (green line), c)  $\text{Fe}(\text{ClO}_4)_2 \cdot 6\text{H}_2\text{O}$  electrolyzed at 0.15 V for 21 min (black line), and **1** upon addition of 1 eq. of  $\text{Fe}(\text{ClO}_4)_3 \cdot 6\text{H}_2\text{O}$  (purple line), d)  $\text{Co}(\text{ClO}_4)_2 \cdot 6\text{H}_2\text{O}$  electrolyzed at 0.26 V for 26 min (black line), and electrochemically generated  $[\text{Cr}^{\text{III}}(\text{F}_4\text{Cat})(\text{F}_4\text{SQ})_2]^-$  (green line), and e)  $\text{Zn}(\text{ClO}_4)_2 \cdot 6\text{H}_2\text{O}$  electrolyzed at 0.20 V for 21 min (black line) and electrochemically generated  $[\text{Cr}^{\text{III}}(\text{F}_4\text{Cat})(\text{F}_4\text{SQ})_2]^-$  (green line), in MeCN using  $n\text{-Bu}_4\text{NPF}_6$  (0.1 M) under an atmosphere of  $\text{N}_2$ .

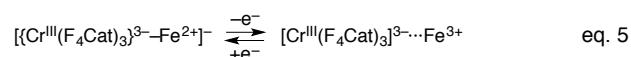
one equivalent of  $\text{Co}^{2+}$  at 0.26 V for 26 min furnished the transient spectrum shown in Figures 11d (black line) and Figure S15. The observed absorption peaks at 381sh., 448sh., 526, 650sh., 710sh., 779sh., and 1830 nm are identical to those of the electrochemically generated  $[\text{Cr}^{\text{III}}(\text{F}_4\text{Cat})(\text{F}_4\text{SQ})_2]^-$  (green line). The formation of the two-electron oxidized species suggests that the first oxidation process at 0.13 V (Figure 10e) should be most likely ascribed to a ligand-centred two-electron oxidation of  $[\{\text{Cr}^{\text{III}}(\text{F}_4\text{Cat})_3\}^3-\text{Co}^{2+}]^-$  (eq. 3).



Electrolysis of **1** in the presence of  $\text{Mn}^{2+}$  or  $\text{Zn}^{2+}$  at 0.12 V for 6 min or 0.20 V for 21 min, respectively, resulted in the emergence of new bands at 390, 538, 714, 775, and 1620 nm ( $\text{Mn}^{2+}$ ), or at 443, 523, 635sh., 715, 795sh., and 1750 nm ( $\text{Zn}^{2+}$ ) as shown in Figures 11b (black line), 11e (black line), S16, and S17. The spectral features are very similar to that of  $[\text{Cr}^{\text{III}}(\text{F}_4\text{Cat})(\text{F}_4\text{SQ})_2]^-$  (green lines in Figures 11b and 11e), suggesting the generation of the two-electron oxidized species of **1**. In addition, similar spectra were obtained by adding one equivalent of  $\text{Mn}^{2+}$  or  $\text{Zn}^{2+}$  to electrochemically generated  $[\text{Cr}^{\text{III}}(\text{F}_4\text{Cat})_2(\text{F}_4\text{SQ})_2]^{2-}$  (Figures S13b and S13c). One reasonable mechanism for the generation of  $[\text{Cr}^{\text{III}}(\text{F}_4\text{Cat})(\text{F}_4\text{SQ})_2]^-$  would be disproportionation of  $[\text{Cr}^{\text{III}}(\text{F}_4\text{Cat})_2(\text{F}_4\text{SQ})_2]^{2-}$  in the presence of  $\text{Mn}^{2+}$  or  $\text{Zn}^{2+}$  (eq. 4).



Electrolysis of **1** at 0.15 V for 21 min in the presence of one equivalent of  $\text{Fe}^{2+}$  generated absorption bands at 507sh., 541, and 715sh. nm (black line in Figure 11c, and S18), while no bands were observed in the NIR region.<sup>30</sup> The absence of any IVCT bands indicates that the RML moiety maintains the original oxidation state of  $[\text{Cr}^{\text{III}}(\text{F}_4\text{Cat})_3]^{3-}$  after the electrolysis. Therefore, oxidation of  $\text{Fe}^{2+}$  bound to the RML is suggested. The iron-centred oxidation process could be confirmed by adding one equivalent of  $\text{Fe}^{3+}$  to a MeCN solution of **1**. After the addition, absorption bands appeared at 507sh., 550, and 722 nm (purple line in Figure 11c, and Figure S19), which can be assigned to ligand-to-metal charge transfer bands ( $\text{Fe}^{3+} \leftarrow \text{F}_4\text{Cat}^{2-}$ ).<sup>31</sup> Therefore,  $\text{Fe}^{2+}$  acts as an active centre for the oxidation of  $[\{\text{Cr}^{\text{III}}(\text{F}_4\text{Cat})_3\}^3-\text{Fe}^{2+}]^-$  (eq. 5).



These results indicate that complex **1** is a ligand-centred RML and that its electron transfer processes can be modulated by the choice of guest metal ion.

## Conclusions

In summary, this paper described the binding interactions between the RML  $[\text{Cr}^{\text{III}}(\text{F}_4\text{Cat})_3]^{3-}$  and the guest metal ions  $\text{Li}^+$ ,  $\text{Mn}^{2+}$ ,  $\text{Fe}^{2+}$ ,  $\text{Co}^{2+}$ ,  $\text{Cu}^{2+}$ , and  $\text{Zn}^{2+}$ . As  $\text{Cu}^{2+}$  is a relatively strong oxidizing agent, the reaction between  $[\text{Cr}^{\text{III}}(\text{F}_4\text{Cat})_3]^{3-}$  and  $\text{Cu}^{2+}$

resulted in the formation of the ligand-centred one-electron oxidized species  $[\text{Cr}^{\text{III}}(\text{F}_4\text{Cat})_2(\text{F}_4\text{SQ})]^{2-}$  and  $\text{Cu}^+$ . However, in the presence of relatively hard and weakly oxidizing metal ions such as  $\text{Li}^+$ ,  $\text{Mn}^{2+}$ ,  $\text{Fe}^{2+}$ ,  $\text{Co}^{2+}$ , and  $\text{Zn}^{2+}$ ,  $[\text{Cr}^{\text{III}}(\text{F}_4\text{Cat})_3]^{3-}$  binds to the guest metal ions *via* the lone pairs on the coordinating oxygen atom(s) of the  $\text{F}_4\text{Cat}^{2-}$  moieties. Furthermore, the present work demonstrated that the redox properties of this RML, *i.e.* oxidation potentials, number of transferred electrons, and redox reaction centres, can be modulated *via* the interactions with the guest metal ions. Our current efforts are focused on revealing the redox properties of guest metal-bound RMLs, as well as on the construction of multi-electron transfer reactions using RMLs as an electron/hole reservoir.

## Acknowledgements

The authors are grateful to Prof. Tamejiro Hiyama and Prof. Yasunori Minami (Chuo Univ.) for their support with the ESI-MS measurements. The authors would also like to thank Prof. Yutaka Hitomi (Doshisha Univ.) for his support with the UV-vis titration experiments. This work was supported by a Grant-in-Aid for Scientific Research (26620050 and 25288024) and a Grant-in-Aid for Scientific Research (B) (23350025) from the Ministry of Education, Culture, Sports, Science and Technology (MEXT), Japan, as well as by a KAKENHI Grant from the JSPS (grant number 26-2494).

## Notes and references

- a) P. Du, R. Eisenberg, *Energy. Environ. Sci.*, 2012, **5**, 6012. b) A. J. Esswein, D. G. Nocera, *Chem. Rev.*, 2007, **107**, 4022. c) J. J. Concepcion, J. W. Jurss, M. K. Brennaman, P. G. Hoertz, A. O. T. Patrocinio, N. Y. M. Iha, J. L. Templeton, T. J. Meyer, *Acc. Chem. Res.*, 2009, **42**, 1954.
- a) S. Günes, H. Neugebauer, N. S. Sariciftci, *Chem. Rev.*, 2007, **107**, 1324. b) R. H. Friend, R. W. Gymer, A. B. Holmes, J. H. Burroughes, R. N. Marks, C. Taliani, D. D. C. Bradley, D. A. D. Santos, J. L. Brédas, M. Löngdlund, W. R. Salaneck, *Nature*, 1999, **397**, 121. c) J. Roncali, *Chem. Rev.*, 1992, **92**, 711.
- a) D. -L. Long, E. Burkholder, L. Cronin, *Chem. Soc. Rev.*, 2007, **36**, 105. b) C. L. Hill, C. M. P.-McCarthy, *Coord. Chem. Rev.*, 1995, **143**, 407. c) M. T. Pope, A. Müller, *Angew. Chem. Int. Ed.*, 1991, **30**, 34.
- a) F. E. Hahn, M. C. Jahnke, *Angew. Chem. Int. Ed.*, 2008, **47**, 3122. b) S. Kitagawa, R. Kitaura, S. Noro, *Angew. Chem. Int. Ed.*, 2004, **43**, 2334. c) B. J. Holloday, C. A. Mirkin, *Angew. Chem. Int. Ed.*, 2001, **40**, 2022.
- a) D. Astruc, *New. J. Chem.*, 2011, **35**, 764. b) C. M. Casado, I. Cuadrado, M. Morán, B. Alonso, B. García, B. González, J. Losada, *Coord. Chem. Rev.*, 1999, **185-186**, 53.
- T. Hamaguchi, H. Nagino, K. Hoki, H. Kido, T. Yamaguchi, B. Breedlove, T. Ito, *Bull. Chem. Soc. Jpn.*, 2005, **78**, 591.
- a) R. F. Munhá, R. A. Zarkesh, A. F. Feyduk, *Dalton Trans.*, 2013, **42**, 3751. b) W. Kaim, B. Schwederski, *Coord. Chem. Rev.*, 2010, **254**, 1580. c) M. D. Ward, J. A. McCleverty, *J. Chem. Soc. Dalton Trans.*, 2002, 275.
- a) M. Costas, M. P. Mehn, M. P. Jensen, L. Que, Jr., *Chem. Rev.* 2004, **104**, 939. b) C. G. Pierpont, R. M. Buchanan, *Coord. Chem. Rev.*, 1981, **38**, 45. c) F. Röhrscheid, A. L. Balch, R. H. Holm, *Inorg. Chem.*, 1966, **5**, 1542.
- a) P. R. Klich, A. T. Daniher, P. R. Challen, D. B. McConville, W. J. Youngs, *Inorg. Chem.*, 1996, **35**, 347. b) B. -S. Kang, M. -C. Hong, T. -B. Wen, H. -Q. Liu, J. -X. Lu, *J. Clust. Sci.*, 1995, **6**, 379. c) B. Kang, L. Weng, H. Liu, D. Wu, L. Huang, C. Lu, J. Cai, X. Chen, J. Lu, *Inorg. Chem.*, 1990, **29**, 4873.
- a) K. Ray, S. D. George, E. I. Solomom, K. Wieghardt, F. Neese, *Chem. Eur. J.*, 2007, **13**, 2783. b) F. E. Hahn, C. S. Isfort, T. Pape, *Angew. Chem. Int. Ed.*, 2004, **43**, 4807. c) N. Robertson, L. Cronin, *Coord. Chem. Rev.*, 2002, **227**, 93.
- a) C. G. Pierpont, *Inorg. Chem.*, 2011, **50**, 9766. b) P. Zanello, M. Corsini, *Coord. Chem. Rev.*, 2006, **250**, 2000.
- a) L. A. deLearie, R. C. Haltiwanger, C. G. Pierpont, *Inorg. Chem.*, 1987, **26**, 817. b) W. P. Griffith, C. A. Pumphrey, T. -A. Rainey, *J. Chem. Soc. Dalton Trans.*, 1986, 1125.
- a) H. -C. Chang, H. Miyasaka, S. Kitagawa, *Inorg. Chem.* 2001, **40**, 146. b) H. -C. Chang, T. Ishii, M. Kondo, S. Kitagawa, *J. Chem. Soc. Dalton Trans.*, 1999, 2467. c) H. H. Downs, R. M. Buchanan, C. G. Pierpont, *Inorg. Chem.* 1979, **18**, 1736.
- a) B. Chen, S. Xiang, G. Qian, *Acc. Chem. Res.*, 2010, **43**, 1115. b) S. R. Halper, L. Do, J. R. Stork, S. M. Cohen, *J. Am. Chem. Soc.*, 2006, **128**, 15255. c) S. Noro, H. Miyasaka, S. Kitagawa, T. Wada, T. Okubo, M. Yamashita, T. Mitani, *Inorg. Chem.*, 2005, **44**, 133.
- a) K. N. Raymond, S. S. Isied, L. D. Brown, F. R. Fronczek, J. H. Nibert, *J. Am. Chem. Soc.*, 1976, **98**, 1767. b) S. R. Cooper, Y. B. Koh, K. N. Raymond, *J. Am. Chem. Soc.*, 1982, **104**, 5092. c) C. J. Rolle III, K. I. Hardcastle, J. D. Soper, *Inorg. Chem.*, 2008, **47**, 1892. d) J. R. Hartman, B. M. Foxman, S. R. Cooper, *Inorg. Chem.*, 1984, **23**, 1381.
- T. Matsumoto, H. -C. Chang, A. Kobayashi, K. Uosaki, M. Kato, *Inorg. Chem.*, 2011, **50**, 2859.
- T. Matsumoto, M. Wakizaka, H. Yano, A. Kobayashi, H. -C. Chang, M. Kato, *Dalton Trans.*, 2012, **41**, 8303.
- a) R. Berger, G. Resnati, P. Metrangolo, E. Weber, J. Hulliger, *Chem. Soc. Rev.*, 2011, **40**, 3496. b) M. Hird, *Chem. Soc. Rev.*, 2007, **36**, 2070. c) N. M. Doherty, N. W. Hoffman, *Chem. Rev.*, 1991, **91**, 553.
- W. Weng, Z. Zhang, J. A. Schlueter, P. C. Redfern, L. A. Curtiss, K. Amine, *J. Power Sources*, 2011, **196**, 2171.
- B. T. Worrell, J. A. Malik, V. V. Fokin, *Science*, 2013, **340**, 457.
- a) S. S. Isied, G. Kuo, K. N. Raymond, *J. Am. Chem. Soc.*, 1976, **98**, 1763. b) S. R. Sofen, D. C. Ware, S. R. Cooper, K. N. Raymond, *Inorg. Chem.*, 1979, **18**, 234.
- a) F. Morishima, R. Kusaka, Y. Inokuchi, T. Haino, T. Ebata, *J. Phys. Chem. B*, 2015, **119**, 2557.
- H. -C. Chang, K. Mochizuki, S. Kitagawa, *Inorg. Chem.* 2002, **41**, 4444.
- C. Reichardt, *Chem. Rev.*, 1994, **94**, 2319.
- D. Ajloo, B. Yoonesi, A. Soleymanpour, *Int. J. Electrochem. Sci.*, 2010, **5**, 459.
- R. G. Pearson, *J. Am. Chem. Soc.*, 1963, **85**, 3533.
- a) J. S. Renny, L. L. Tomasevich, E. H. Tallmadge, D. B. Collum, *Angew. Chem. Int. Ed.*, 2013, **52**, 11998. b) G. M. Dykes, D. K. Smith, *Tetrahedron*, 2003, **59**, 3999. c) S. C. Zimmerman, W. Wu, Z. Zeng, *J. Am. Chem. Soc.*, 1991, **113**, 196.
- a) K. Hirose, *J. Incl. Phenom. Macrocycl. Chem.*, 2001, **39**, 193. b) H. -J. Böhm, *J. Comput. Aid. Mol. Des.*, 1994, **8**, 243. c) H. -J. Schneider, *Angew. Chem. Int. Ed.* 1991, **30**, 1417. d) K. A. Connors, *Binding Constants:*

- The Measurements of Molecular Complex Stability*, John Wiley + Sons, 1987.
- 29 C. Ikeda, S. Ueda, T. Nabeshima, *Chem. Commun.*, 2009, 2544.
- 30 Electrolysis at  $-0.4$  V furnished the original spectrum, supporting the reversibility of the oxidation process (Figure S18b).
- 31 a) Y. Hitomi, M. Yoshida, M. Higuchi, H. Minami, T. Tanaka, T. Funabiki, *J. Inorg. Biochem.*, 2005, **99**, 755.  
b) A. Dei, D. Gatteschi, L. Pardi, *Inorg. Chem.*, 1993, **32**, 1389. c) H. G. Jang, D. D. Cox, L. Que, Jr., *J. Am. Chem. Soc.*, 1991, **113**, 9200.

## Table of Contents Entry

The interaction between  $[\text{Cr}^{\text{III}}(\text{F}_4\text{Cat})_3]^{3-}$  ( $\text{F}_4\text{Cat}$  = perfluorocatecholato), redox-active metalloligand (RML), that exhibits three-step one-electron transfer ability on ligand-centered, and guest metal ions in MeCN is discussed. While  $[\text{Cr}^{\text{III}}(\text{F}_4\text{Cat})_3]^{3-}$  binds to guest metal ions such as  $\text{Li}^+$ ,  $\text{Mn}^{2+}$ ,  $\text{Fe}^{2+}$ ,  $\text{Co}^{2+}$ , and  $\text{Zn}^{2+}$ , it engages in redox reactions with  $\text{Cu}^{2+}$ , which demonstrates a remarkable selectivity towards the guest metal ions. This study thus demonstrates systematic ability of  $[\text{Cr}^{\text{III}}(\text{F}_4\text{Cat})_3]^{3-}$  to act as a RML in solution for the first time.

